ELSEVIER

International Journal of Mass Spectrometry 216 (2002) 95–113

International Journal of Mass Spectrometry

www.elsevier.com/locate/ijms

Determination of atomic isotope patterns from mass spectra of molecular ions containing multiple polyisotopic elements

José G.A. Brito-Neto, Claudimir L. do Lago*

Instituto de Química, Universidade de São Paulo, Av. Prof. Lineu Prestes 748, São Paulo, SP, CEP 05508-900, Brazil

Received 9 October 2001; accepted 24 January 2002

Abstract

A chemometrical method that allows one to obtain the isotopic abundances of the atoms composing a molecular ion, given its elemental composition and its mass spectrum, was developed. The method uses non-linear regression to fit the isotopic abundances of the elements, so that the experimental spectrum of the ion is reproduced. A least squares method with minimization by downhill simplex algorithm was implemented in C language as a library, but a graphical user interface application that allows an end-user to apply the method to his/her own spectra is also available. Examples of its application to electrospray mass spectra of $NaAuCl_4$ and $CdCl_2$ are given. The chlorine isotope pattern was obtained from the $AuCl_4^-$ cluster in the former case and, simultaneously, chlorine and cadmium isotope patterns from the $CdCl_3^-$ cluster. The performance of the method was extensively characterized by applying it to a great number of simulated spectra. Non-idealities, against which the method was evaluated, include noise, mass discrimination, detection non-linearity, base line offset (background counting), and low resolution. It has been demonstrated that, in spite of what intuition might tell one, the polyatomic approach to isotopic analyses has no a priori disadvantage to the common monatomic approach. Indeed, the results demonstrate that, in some cases, the figures of merit can be improved by using polyatomic species and that other polyisotopic elements can be included in the formula without significant loss of precision, as long as they have a dominant isotope, which is the case of carbon, hydrogen, oxygen, and nitrogen, for example. This means that polyatomic species derived from organic species could be useful for isotopic measurement purposes. (Int J Mass Spectrom 216 (2002) 95–113)

Keywords: Isotopic ratio; Isotope pattern; Chemometrics; Deconvolution; Electrospray

1. Introduction

One of the aims of mass spectrometry is to determine isotopic compositions. There are several applications for such data in many different areas, such as nuclear energy, geology, nutrition, and environmental studies.

Typically elemental ions or simple polyatomic ions containing the element of interest are generated in the ion source. Ion beam intensities are measured over a time interval long enough to attain the desired precision. From these measurements, one can obtain the abundance ratio, which is the most commonly used piece of information in the above-cited applications.

For elemental ions, peak intensities are directly associated with isotopic abundances. However, if polyatomic ions are used, the contributions of all nuclides involved in the composition of the ion must be considered.

* Corresponding author. E-mail: claudemi@iq.usp.br

1387-3806/02/$ – see front matter
PII S1387-3806(02)00555-9

Isotopic patterns are often obtained by destroying the molecules, reducing them to elemental ions or oxides. Several such approaches have been proposed, which use inductively coupled plasma (ICP-MS) [1], combustion followed by electron impact ionization [2], or thermal ionization (TIMS) [3]. Following molecular destruction, the desired isotopic patterns can be directly measured. For oxides, the interference of oxygen can be manually corrected, such as for $Na_2BO_2^+$ or $Cs_2BO_2^+$ obtained by positive thermal ionization [4,5]. Although sodium is monoisotopic, oxygen has three stable isotopes, which cause isobaric interference: for example, $^{23}Na_2{}^{11}B^{16}O_2^+$ has the same integer mass as $^{23}Na_2{}^{10}B^{17}O^{16}O^+$. After data acquisition, this isobaric interference must be mathematically compensated to obtain the unbiased boron isotopic ratio. Other similar examples include $SO_2^{\bullet+}$ for sulfur, $N_2^{\bullet+}$ for nitrogen, and $CO_2^{\bullet+}$ for carbon and oxygen.

One approach to avoid this sort of isobaric interference is to use species in which the only polyisotopic element is the desired one, for example S in $SF_6^{\bullet+}$, and Fe in FeF_4^-. The former is obtained by ionization of gaseous SF_6, while the latter is generated by negative thermal ionization of a fluoride-containing Fe sample. The use of monoisotopic fluoride and iodide ligands has also been proposed for the generation of anionic complexes of metals and boron by electrospray [6].

The isobaric interference of species with different formulas is a more complicated case, because its mathematical compensation is not necessarily trivial. Normally, the solution is to turn to another technique and/or chemical species. For example, iron suffers interference with ArO^+ in ICP-MS. Alternatively, it can be analyzed as FeF_4^- by TIMS, or as $Fe(PF_3)_5$ by electron impact [7].

An advantage of the use of polyatomic species for mass analysis is the shift towards higher masses. Thus, isotopic fractionation due to instrumental mass discrimination can be diminished for lighter elements [8]. For example, $Cs_2BO_2^+$ is more convenient than $Na_2BO_2^+$, because cesium is heavier than sodium. Moreover, higher masses are less prone to isobaric interference.

Sample preparation may be laborious, however. Chlorine can be ionized via electron impact of CH_3Cl, which produces Cl^+. However, chlorine from a generic source must first be converted to methyl chloride, which requires several synthesis steps [9]. Similarly, syntheses of SF_6 and $Fe(PF_3)_5$ are also laborious [6,7].

From these considerations, one can note that, even though there exist methods for isotopic abundance determination for most elements, new methods with increased precision and accuracy (e.g., by elimination of isobaric interference or diminishment of isotopic fractionation and instrumental mass discrimination), simplified sample handling, and/or reduced cost, are still being looked for. Most efforts in this direction are devoted to improvements in instrumentation and sample preparation. However, chemometric algorithms can be envisioned as post-treatment procedures to improve the quality of the extracted information. Although mathematical methods are being routinely used for tasks such as compensating detector dead time, instrumental mass discrimination, and the interference of the oxygen isotopes in the element oxide ion (e.g., $CO_2^{\bullet+}$, $SO_2^{\bullet+}$, and $Na_2BO_2^+$), more sophisticated approaches can be used. For example, $^6Li/^7Li$ and/or $^{10}B/^{11}B$ can be analyzed through the $Li_2BO_2^+$ ion in TIMS as suggested by Datta and coworkers [10–14].

In this paper we introduce a mathematical method (IPDec) to obtain the isotopic patterns of the elements that compose a polyatomic ion given its isotopomeric pattern and elemental composition. This method allows one to obtain the isotopic pattern of an element by using a species containing several polyisotopic atoms, thus broadening the universe of usable polyatomic species beyond simple oxides and fluorides.

2. Mathematical method

The purpose of this method is to find the set of elemental isotopic patterns that, given the formula of a molecular ion, produce an isotopomeric pattern that best fits an experimental mass spectrum. In order to do so, one needs two basic components: (a) a general way to calculate the isotopomeric pattern of a molecule

given its elemental composition and the isotopic patterns of its constituent atoms, and (b) a way to adjust these atomic isotopic patterns so that the calculated isotopomeric pattern approximates the experimentally measured one.

Considering zero width peaks (infinite resolution) separated by exactly one mass unit, and that the lightest isotope has zero mass, one can calculate the isotopomeric pattern by polynomial expansion [15]. In this approach, the patterns are represented by polynomials whose coefficients are the isotopic/isotopomeric abundances.

$$P(a; x) = \sum_{i=1}^{N_p} a_i x^{i-1} \tag{1}$$

where N_p is the number of peaks in the pattern and the a_i is the abundance of the ith peak ordered by mass. For example, the chlorine isotopic pattern can be represented by the polynomial of Eq. (1) with $a^T = (0.7577\,0\,0.2423)$.

The multiplication of the polynomials associated with the elemental isotopic patterns raised to their formula numbers yields the molecular isotopomeric pattern

$$P_C(\boldsymbol{A}; x) = \prod_{i=1}^{N_E} P_i(\boldsymbol{A}^{\langle i\rangle}; x)^{v_i} \tag{2}$$

where $\boldsymbol{A}$ is a matrix whose ith column ($\boldsymbol{A}^{\langle i\rangle}$) contains the isotopic abundances of the ith element, v_i is its formula number, and N_E is the number of different elements in the formula. For example, the matrix $\boldsymbol{A}$ for the $CdCl_3^-$ ion is

$$\boldsymbol{A}^T = \begin{bmatrix} 0.0125 & 0 & 0.0089 & 0 & 0.1249 & 0.1280 & 0.2413 & 0.1222 & 0.2873 & 0 & 0.0749 \\ 0.7577 & 0 & 0.2423 & 0 & 0 & 0 & 0 & 0 & 0 & 0 & 0 \end{bmatrix}$$

If adequately implemented, this infinite resolution polynomial expansion is reasonably fast and gives very good results for small to medium-sized molecules.

The function to be minimized by varying the atomic isotopic abundance is

$$S(\boldsymbol{A}; \boldsymbol{I}) = \sum_{i=1}^{N} (k \cdot Y_i - I_i)^2 \tag{3}$$

where $\boldsymbol{I}$ is the vector of experimental intensities, N the number of peaks of the calculated isotopomeric pattern, and Y_i is the coefficient of the x^{i-1} term of the P_C polynomial (which corresponds to the ith peak of the calculated isotopomeric pattern). The variable k is a scaling factor given by

$$k = \frac{\sum_{i=1}^{N} Y_i I_i}{\sum_{i=1}^{N} Y_i^2} \tag{4}$$

that has the same units as the experimental intensities, and fits the isotopomeric pattern to the experimental spectrum by least squares.

In summary, the elements of the $\boldsymbol{A}$ matrix are varied, the polynomial P_C, the scale factor k and then the function S are evaluated. The process is repeated until S is minimized. The success or failure of the method depends on the manner by which the elements of the $\boldsymbol{A}$ matrix are varied.

3. Implementation

For minimization, we chose the downhill simplex algorithm, due to its simplicity and versatility [16]. Although gradient methods are more efficient with respect to the number of function evaluations necessary, the calculation of the derivatives of S with respect to the isotopic abundances being adjusted is time consuming and can be a source of error for large formulas.

The method was implemented in C as a library, and can be used in other programs. It was compiled with the GNU C Compiler version 2.95.2 under Linux (Debian 2.2, kernel version 2.2.14) and MS-Windows 95/98. The program must provide the library with the spectrum to be fitted, formula numbers of the elements to be considered, and the initial estimates of their isotopic patterns.

The library is used in an analysis module of a graphical software package written in-house for the

manipulation of mass-spectral data. This program uses the GTK+ graphical toolkit, and can be obtained from the authors in source C form upon request. Pre-compiled binaries for MS-Windows 95/98 and Linux are also available.

The implementation allows one to choose which isotopic abundances should be adjusted, and which must remain fixed. This feature is useful for elements like bromine, whose 80-isotope has zero abundance. Another case in which this feature is useful is when one knows a priori the isotopic pattern of an element, such as when one wishes to correct for the interference of the oxygen isotopic pattern over the isotopic pattern of another element.

A binary mask can be used to select a subset of the experimental peaks to be considered in the regression. This feature can be used to disregard some of the experimental peaks when one knows that they are subject to some isobaric interference.

The polynomial expansion was implemented using a binary construction scheme as described by Kubinyi [15], but without any disregarding threshold. This method is reasonably fast and accurate for small to medium-sized molecules.

Since the isotopic abundances are calculated by an iterative non-linear regression algorithm, statistical dispersion information is not easily obtained. The simplest ways to perform the error propagation from the experimental spectrum to the elemental isotopic abundances are as follows:

1. when the user has access to a set of repeated measurements of the experimental spectrum, the method can be applied to each spectrum in this set individually and the results consolidated at the end;
2. when the user has some information about the probability distribution of the experimental spectrum, the Monte Carlo method can be employed to do the propagation. Pseudo-random spectra with the known probability distribution are generated, the method is applied to each of them, and the results are consolidated to obtain statistical information about the isotopic abundances.

4. Results and discussion

From the description of the method, one should note that its application is not restricted to a single type of mass spectrometer, or chemical species. In fact, this method is valid whenever one has a mass spectrum of a known polyatomic species. However, since the mathematical method is not intuitive, some demonstration of its usability and performance is needed to convince the reader that he/she should consider this approach to develop new methods of isotopic measurement. Before proceeding to the systematic exploration of the characteristics of the method, we present some examples of its application to experimental and simulated spectra, so that the reader can get acquainted with the sorts of possibilities it opens.

In this first example, the method is applied to the cluster of the $AuCl_4^-$ ion, obtained by electrospray ionization of a 100 μM $NaAuCl_4$ solution in methanol/swater 99:1. Experimental details can be found elsewhere [6]. This example is interesting, because gold is monoisotopic and, thus, the observed isotopomeric pattern is that of four chlorine atoms.

Fig. 1 contains the base peak normalized experimental spectrum. The inset contains the calculated chlorine isotopic pattern, as well as its tabulated natural isotopic abundances. In this regression, the abundance of the ^{36}Cl isotope was kept constant and equal to zero.

The $CdCl_3^-$ ion provides a more dramatic example of application of the method. Both constituent elements of this ion are polyisotopic, and cadmium has a very complex isotopic pattern encompassing 11 mass units.

Fig. 2 contains the base peak normalized electrospray spectrum of $CdCl_3^-$ obtained from a 100 μM $CdCl_2$ solution in methanol/water 99:1. Experimental details can be found in [6]. Fig. 3 contains the adjusted isotopic patterns of cadmium and chlorine, as well as the natural abundances. In this regression, the abundances of ^{107}Cd, ^{109}Cd, ^{115}Cd, and ^{36}Cl were kept constant and equal to zero.

In these two examples, only semi-quantitative concordance between the tabulated natural isotopic

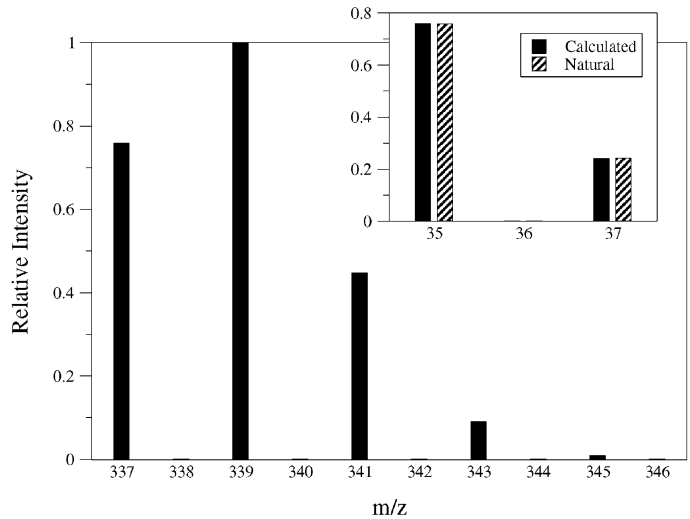

Fig. 1. Experimental electrospray ionization mass spectrum of a 100 μM $NaAuCl_4$ solution in methanol/water 99:1. The inset shows the calculated chlorine isotopic pattern (black), as well as its tabulated natural isotopic abundances (hachured).

abundances and the calculated ones was achieved. There is no sense in expecting more than a qualitative agreement in these cases, because no procedures for compensation of instrumental mass discrimination and other systematic experimental errors were performed, nor were isotopically certified samples used. These examples simply demonstrate some of the general features and possible applications for the method. In the next sections we will present a systematic study of its performance.

Isotopic abundances, peak intensities, and noise are parameters that can be freely chosen when simulated data are produced. However, in actual spectra these parameters depend on a set of conditions that are not

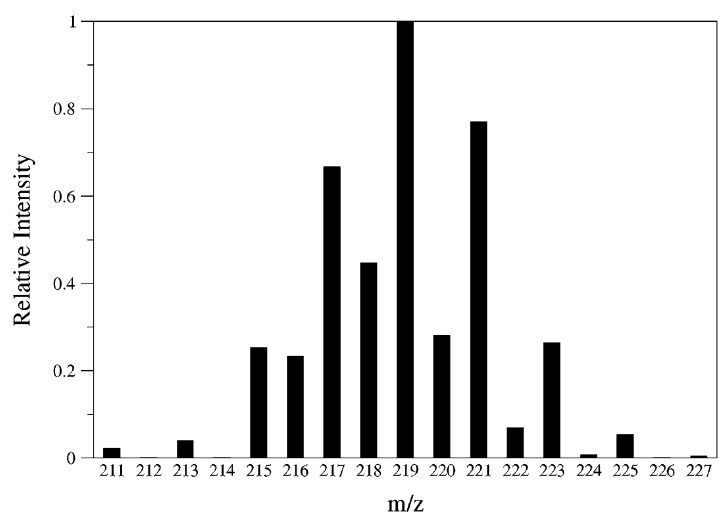

Fig. 2. Experimental electrospray ionization mass spectrum of a 100 μM $CdCl_2$ solution in methanol/water 99:1.

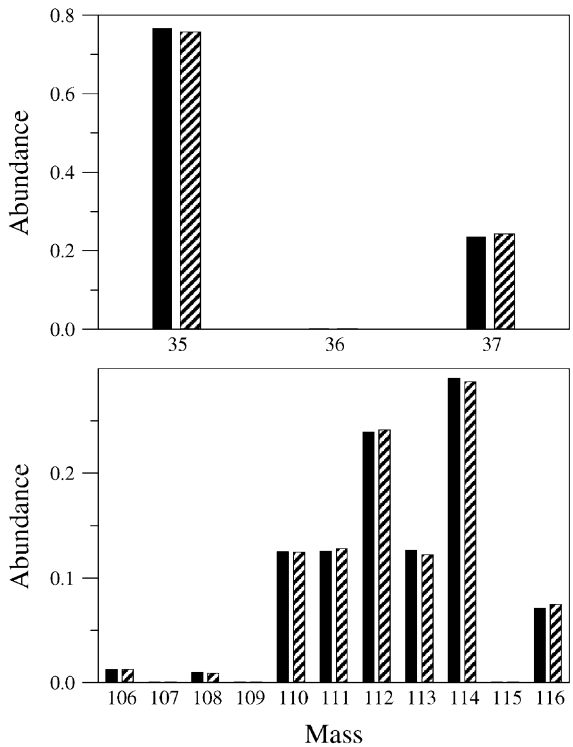

Fig. 3. Calculated (black) and natural (hachured) isotopic patterns of chlorine (top) and cadmium (bottom) based on the spectrum from Fig. 2.

completely under user control. Applying the method to a specific situation may lead to tendentious conclusions, because a favorable or unfavorable case can be selected. Thus, we decided to simulate a large number of spectra with different conditions in order to examine some trends. Based on these, one can envision possible applications for the method. The aspects treated in this paper are noise, resolution, mass discrimination, detection non-linearity, and baseline correction.

For resolution and mass discrimination studies, absolute intensity and signal-to-noise ratio are not important. However, to compare the remaining issues for different formula ions, some sort of normalization is necessary. In all cases, the intensities of the base peaks of the clusters were made equal.

In a first step, hypothetical molecules composed of one or more atoms of a single hypothetical element (A) with two isotopes (^{m}A and $^{m+1}$A) were considered. Besides molecules of the kind A_p, the model can also represent the case of molecules of the type A_pX_q, where X stands for a monoisotopic element.

In a second step, molecules of formula A_pX_q, where X is also polyisotopic, were considered. In this case, the element A has two isotopes: ^{m}A and $^{m+2}$A, and X has two isotopes: $^{m'}$X and $^{m'+1}X$. These isotopic patterns were chosen in order to represent cases such as ions from organochlorine compounds. The isotope patterns of both elements were adjusted, i.e., no restriction was placed on the method.

5. The case of molecules with one polyisotopic element

5.1. Noise

As any other kind of measurement, isotopic abundances are affected by noise. There are basically two types of peak intensity measurement modes: ion counting (digital) and continuous current (analog). Ion counting data follow Poisson statistics, and are intrinsically heteroscedastic. Analog signals are more complex, because, although the original signal is related to the ion counting statistics, there is also a contribution from electronic circuit noise (white noise). The resulting behavior may be heteroscedastic or homoscedastic, and the probability distribution approaches the normal one.

The way in which noise propagates from the experimental spectra to the method results was explored using the Monte Carlo method. To do so, thousands of spectra were simulated considering that their peaks had some a priori known probability distribution, the method was applied to each, and the results were consolidated at the end.

Obviously, as the formula number increases, the number of isotopomeric peaks also increases and, thus, the time required to scan all peaks of the cluster increases. Usually, a stable signal cannot be maintained indefinitely (i.e., the time available for the measurement is finite), therefore one has to reduce the time

spent for data acquisition. For example, if the experimental signal is stable for 10 min and two peaks are monitored, one can spend only 5 min on each peak. On the other hand, if four peaks are monitored, only 2.5 min can be spent on each. Consequently, in the two-peak case, one will have roughly twice as many scans (spectra) as in the four-peak case. This results in an increase of the standard deviation of the mean by a factor of $2^{1/2}$.

For comparisons of the results obtained with different formula numbers, we assume that measurement time available is finite. This translates into larger apparent standard deviations for the larger formula number clusters. To account for this, every estimated standard deviation (ESD) was multiplied by $(N/n)^{1/2}$, where N is the number of peaks in the isotopomeric pattern, and n the minimum number of peaks (i.e., the number of isotopes).

Two cases were studied: (1) normal heteroscedastic errors with 1‰ relative standard deviation, and (2) normal homoscedastic errors with standard deviation equal to 1‰ of the base peak intensity.

Fig. 4 shows the relative estimated standard deviation (RESD) of the calculated isotopic ratio ($^{m}\mathrm{A}/^{m+1}\mathrm{A}$) as a function of the actual abundance of $^{m}\mathrm{A}$ and formula number. Each point was calculated from 1000 simulated spectra, and each peak was assumed to have an independent normal distribution with 1‰ standard deviation (Case 1: heteroscedastic data). The IPDec method was applied to each spectrum, and the resulting set of abundances was consolidated.

In this case, for elemental ions (formula number = 1), the RESD is constant along the whole abundance range. For polyatomic compositions, the RESD produced by the IPDec method becomes dependent on the isotopic abundances. These results suggest that the use of the polyatomic species and the IPDec method is advantageous for isotopically rich elements (the middle of the abundance range).

Fig. 5 shows the RESD of the calculated isotopic ratio ($^{m}\mathrm{A}/^{m+1}\mathrm{A}$) as a function of the actual $^{m}\mathrm{A}$ abundance for some formula numbers considering homoscedastic data. The isotopic measurement is less precise for quasi-monoisotopic elements, regardless of the formula number. However, a precision improvement by using polyatomic species and IPDec method is achieved.

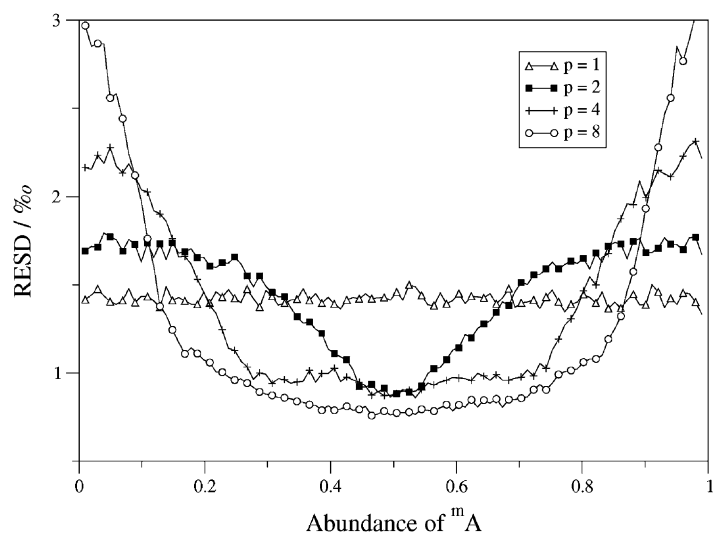

Fig. 4. RESD of the calculated isotopic ratio ($^{m}\mathrm{A}/^{m+1}\mathrm{A}$) as a function of the actual abundance of $^{m}\mathrm{A}$ for formulas A_p. Each point was calculated over 1000 simulated spectra considering that each peak had an independent normal distribution with 1‰ standard deviation (heteroscedastic data).

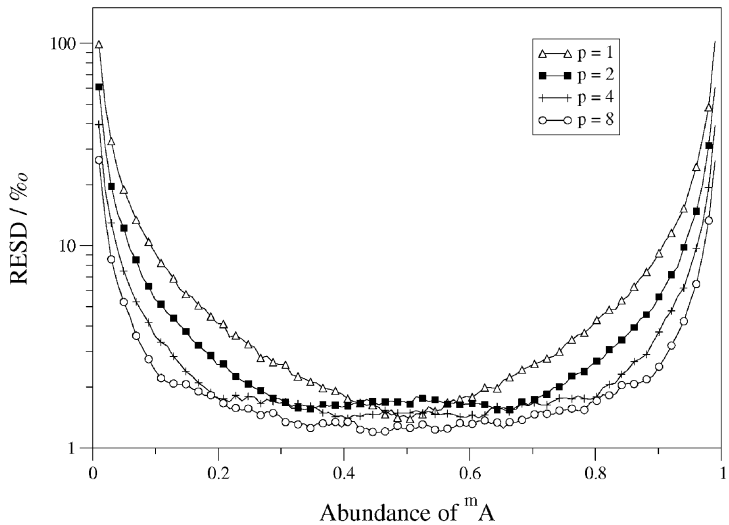

Fig. 5. RESD of the calculated isotopic ratio ($^{m}A/^{m+1}A$) as a function of the actual abundance of ^{m}A for formulas A_p. Each point was calculated over 1000 simulated spectra considering that each peak had an independent normal distribution with standard deviation equal to 1‰ of the base peak intensity (homoscedastic data).

5.2. Instrumental mass discrimination

It is a systematic error in isotopic analyses that occurs due to a difference in the sensitivity of the mass spectrometer (ion production, detector sensitivity, or m/z filter transmission) to different-mass ions. It is a major concern for isotopic analyses and, thus, must be treated here.

Several approaches have been proposed to model instrumental mass discrimination. Among these, three empirical models have had the most success in compensating this bias. These models postulate linear, power, or exponential dependence of the sensitivity on the mass [17]. While the power and exponential laws are mathematically equivalent, the linear law can be considered a special case for narrow mass spans. Thus, only the exponential mass discrimination is treated here. In this model, the measured intensity of a peak is given by

$$I_m = T_m \, \mathrm{e}^{\alpha(m-m_0)} \tag{5}$$

where T_m is the true intensity of the peak m, α is an empirical discrimination constant, and m_0 is an m/z value chosen as reference. The constant α can be either positive or negative when the measured intensities tend to either grow or shrink, respectively, with increasing m/z. Here, the lowest-mass peak of each cluster was chosen as reference, and a 1% increase of sensitivity per mass unit ($\alpha = 9.95 \times 10^{-3}$) was used.

In order to evaluate the effects of systematic errors, the per-thousand relative deviation (δr) of the calculated isotopic ratio relative to its expected value is used

$$\delta r = \frac{1000(r - r_0)}{r_0} \tag{6}$$

For all abundances and formula numbers, δr was equal to -9.901. For modeled isotopic ratio measurements, mass discrimination effects are as significant for large molecules as they are for small molecules. The result for negative α is similar, but with a positive deviation.

As a matter of fact, studies by Held and Taylor [18] have shown that the mass discrimination tends to be smaller for large m/z than for small m/z. This suggests that the method is advantageous, because the use of polyatomic species naturally leads to high m/z values.

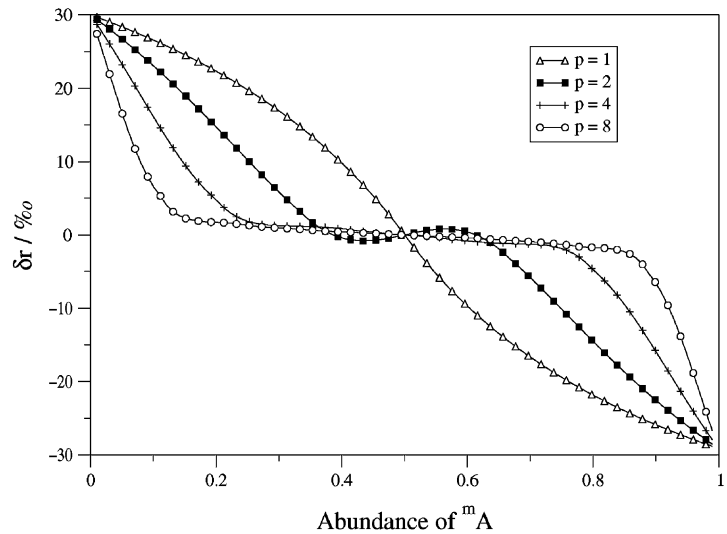

Fig. 6. Effect of the detector dead time on the isotopic ratio for formulas A_p. Base peak intensity is equal to 1 and $\tau = 0.03$ (time units).

5.3. Detection non-linearity

The detectors commonly used in mass spectrometry are not perfectly linear, and variations in ion flux at the detector may not result in a perfectly proportional variation of the recorded signal.

The commonest one of such imperfections is called "detector dead time." It is significant at high counting rates, and results in the recording of smaller than expected intensities. It happens because the detector becomes insensitive for a small period of time after the arrival of an ion.

This effect is empirically modeled by considering that the measured ion intensity is given by

$$I = \frac{T}{1 + \tau T} \tag{7}$$

where τ is the detector dead time, given in time units, and T is the true intensity, given in frequency units ($[\text{time}]^{-1}$) [18].

The value of τ must be chosen so that the product τT, in the right-hand-side of Eq. (7) has a desired value. Since each cluster is scaled so that its base peak has unit intensity, we chose $\tau = 0.03$ (time units), which corresponds to a 30 ns dead time for a 10^6 Hz peak intensity, a value observed with common detectors.

Fig. 6 has the per-thousand deviation of the calculated isotopic ratio from its expected value as a function of the actual ^{m}A abundance and for some formula numbers. It is interesting to note that detector non-linearity is more problematic when the element is quasi-monoisotopic, and zero when both isotopes have the same abundance. This is expected, because peaks of the same intensities have equal ion counting rates. Increasing the formula number, the region around abundance 0.5, in which the non-linearity effect is small, is enlarged. Thus, the model suggests that the polyatomic approach minimizes detector non-linearity effects for a broad range of abundances.

5.4. Base line correction

In ion counting detection, there is a residual production of spurious pulses background. These spurious background pulses are produced continuously, and the residual value should be subtracted from the measured signal. For analog-mode detection, there is a base line due to the electronic signal processing that can assume a value in a broad range in voltage. In both cases, the

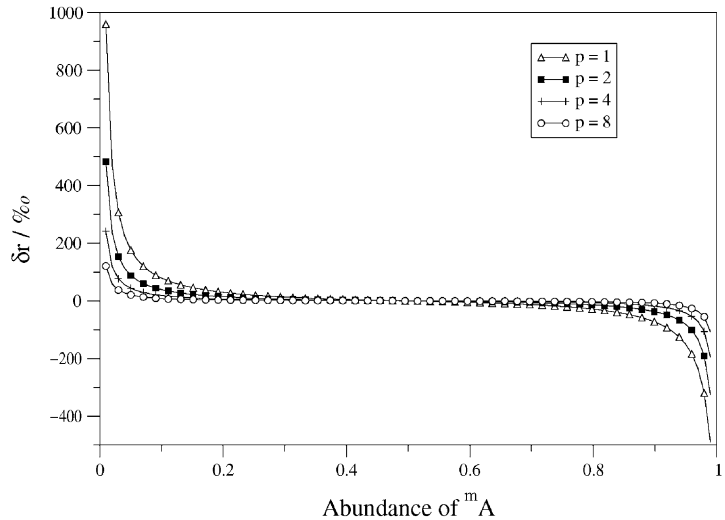

Fig. 7. Effect of the base line on the isotopic ratio for formulas A_p. Base peak intensity is equal to 1 and base line offset is 0.01.

base line must be judiciously compensated, because incorrect base line attribution can lead to systematic errors.

Fig. 7 shows the per-thousand relative deviation of the calculated isotopic ratio from its expected value as a function of the actual ^{m}A abundance for some formula numbers and a 0.01 offset applied to all peaks. The same absolute trend is observed when a negative base line is considered.

The elemental ion isotope pattern is more affected by error in base line attribution when it tends to be monoisotopic. Of course, when both isotopes have exactly the same abundance (0.5), errors in base line are insignificant. The results shown in Fig. 7 suggest that the polyatomic approach is less affected by base line attribution errors.

5.5. Resolution

Although it is possible to obtain high resolution mass spectra, that permit the identification of peaks within a thousandth of a mass unit, the equipments are expensive and, frequently, high resolution is obtained at the expense of ion transmission, which then reduces the signal-to-noise ratio. Thus, less expensive high-transmission, low resolution instruments are commonly used. However, low resolution may lead to errors due to the mutual superimposition of the tails of neighbor peaks.

Fig. 8 shows the per-thousand relative deviation of the calculated isotopic ratio from its expected value as a function of the actual ^{m}A abundance for low resolution spectra. Spectra were simulated as linear combinations of Gaussian-shaped peaks with σ equal to 0.25 u. The inset in Fig. 8 shows the spectrum of A_5 for ^{m}A abundance 0.8, so that the reader can have an idea of the type of peak shape considered. The intensities were calculated by integrating the continuous spectrum within a 0.1 u margin around the nominal *m*/*z*. This example shows a very poor resolution case for illustrative purposes.

Again, quasi-monoisotopic elements are more prone to errors due to the low resolution. In this case, the tail of the higher peak introduces a significant systematic error to the intensity of the lower one. Of course, the mutual interference of equally intense peaks is less significant.

Once again, the polyatomic approach seems to be a better solution. Actually, this is expected, because an isotopomeric distribution approaches a Gaussian curve for large formula numbers [19,20]. In this case, neighbor peaks tend to have similar intensities and,

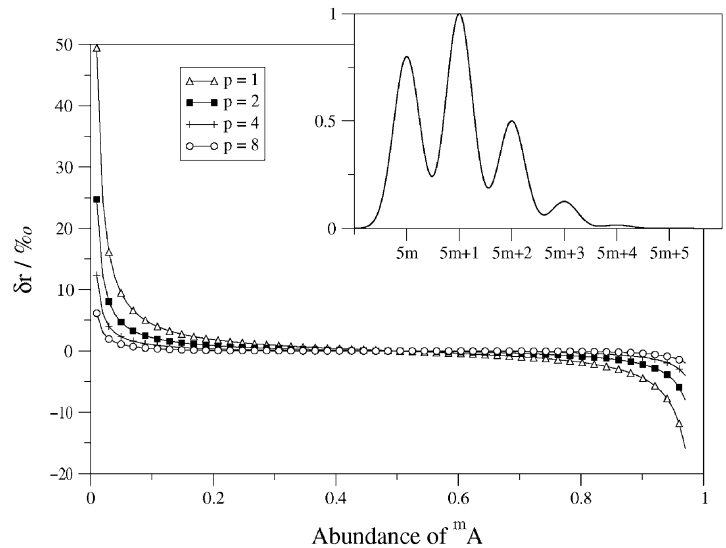

Fig. 8. Effect of the resolution on the isotopic ratio for formulas A_p. Inset shows the simulated spectrum of A_5 with abundance of ^{m}A equal to 0.8.

thus, the mutual interference of the tail tends to be insignificant.

6. The case of molecules with two polyisotopic elements

6.1. Noise

Figs. 9 and 10 show density maps with the RESD obtained in the same way as in the single-element cases of, respectively, homoscedastic and heteroscedastic data. Each map describes the RESD of the isotopic ratio as a function of the actual ^{m}A and $^{m'}X$ abundances for molecules A_5X_5, AX_5, A_5X, and AX.

These results for A_pX_q species can be summarized by: (1) large numbers of A atoms improve the precision of the measured abundance of ^{m}A and (2) the inclusion of the X element can be deleterious if it is isotopically rich.

It is important to note that, for $^{m'}X$ abundance above 0.9 or below 0.1, the results tend to those of the monoisotopic case. This means that, even if X is polyisotopic, the precision of the isotopic ratio measured with molecules of the kind A_pX_q may be better than that obtained by using a lone A atom. Since elements such as carbon, nitrogen, oxygen, and hydrogen belong to this quasi-monoisotopic group, fragments and molecular ions of organic compounds containing the element A, even with high q/p ratio, can be suitable for the IPDec method. In this case, the X element would be used to aggregate a large number of A atoms. For example, a species such as Cl_3^+ cannot be obtained by electron impact, but an organochlorine ion containing several chlorine atoms, such as $C_2H_2Cl_3^+$, can be easily produced by the same technique.

6.2. Instrumental mass discrimination

The per-thousand relative deviation of the calculated isotopic ratio from its expected value is equal to -19.704 for all the expected ^{m}A and $^{m'}X$ abundances and formulas A_pX_q for a equal to 9.95×10^{-3}, which corresponds to a 1% increase of intensity per mass unit. In the same way as observed for the monoelemental case, determinations using larger molecules are affected by mass discrimination in not a larger extent than those using smaller ones. Moreover, the

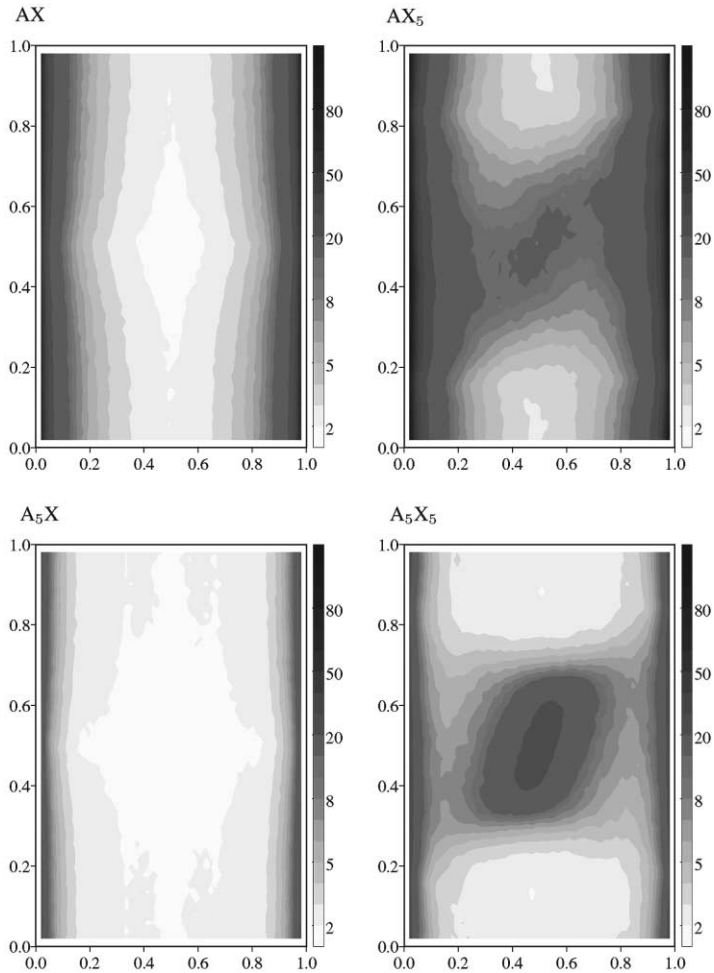

Fig. 9. RESD of the calculated isotopic ratio ($^{m}A/^{m+1}A$) as a function of the actual abundance of ^{m}A (horizontal axis) and $^{m'}X$ (vertical axis). The bar next to each graph maps RESD into a gray scale. Each point was calculated over 1000 simulated spectra considering that each peak had an independent normal distribution with standard deviation equal to 1‰ of the base peak intensity (homoscedastic data).

isotopic pattern of X has no effect, i.e., it does not matter whether X is mono or polyisotopic. Again, the result for negative α is similar, but with a positive deviation, and the m/z is shifted to high mass region by including the element X, which may be advantageous to minimize instrumental mass discrimination.

6.3. Detection non-linearity

Fig. 11 encloses four contour maps with the absolute per-thousand deviation of the calculated A isotopic ratio from its expected value as a function of the actual ^{m}A and $^{m'}X$ abundances for molecules A_5X, AX, AX_5, and A_5X_5. Each cluster is scaled so that its base peak has unit intensity and τ is equal to 0.03 (time units).

When the abundance of $^{m'}X$ tends to 0 or 1, a monoisotopic case of X is achieved and the results tend to that previously discussed. On the other hand, the increasing abundance of a second isotope of the element X tends to produce disturbances in the pattern of A. Although the particular case of abundances equal to

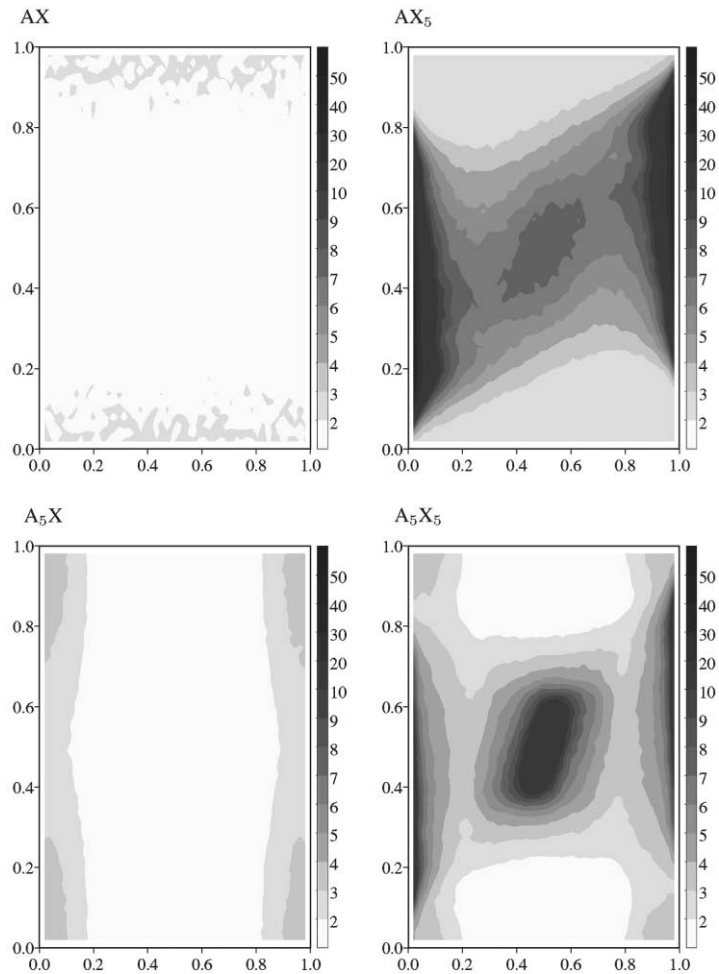

Fig. 10. RESD of the calculated isotopic ratio ($^{m}\mathrm{A}/^{m+1}\mathrm{A}$) as a function of the actual abundance of $^{m}\mathrm{A}$ (horizontal axis) and $^{m'}\mathrm{X}$ (vertical axis). The bar next to each graph maps RESD into a gray scale. Each point was calculated over 1000 simulated spectra considering that each peak had an independent normal distribution with 1‰ standard deviation (heteroscedastic data).

0.5 for both elements is not affected by the detection non-linearity, this region is very sensitive to changes in the abundances. Moreover, for the case $\mathrm{A}_p\mathrm{X}_q$ considered here, the disturbance caused by the non-linearity increases with the q/p ratio. Thus, non-linearity is an issue that must be carefully evaluated for high q/p ratio.

The same comment drawn in the noise evaluation section about the inclusion of isotopically poor elements, such as C, N, H, and O, is also valid here.

6.4. Base line correction

Fig. 12 encloses four contour maps with the absolute per-thousand deviation of the calculated A isotopic ratio from its expected value as a function of the actual $^{m}\mathrm{A}$ and $^{m'}\mathrm{X}$ abundances for molecules $\mathrm{A_5X}$, AX, $\mathrm{AX_5}$, and $\mathrm{A_5X_5}$ and a 0.01 offset applied to all peaks. The trend is the same as the one observed when considering the non-linearity effect, i.e., as long as the X element is not isotopically rich, it can be advantageous to employ species with one or more X atoms.

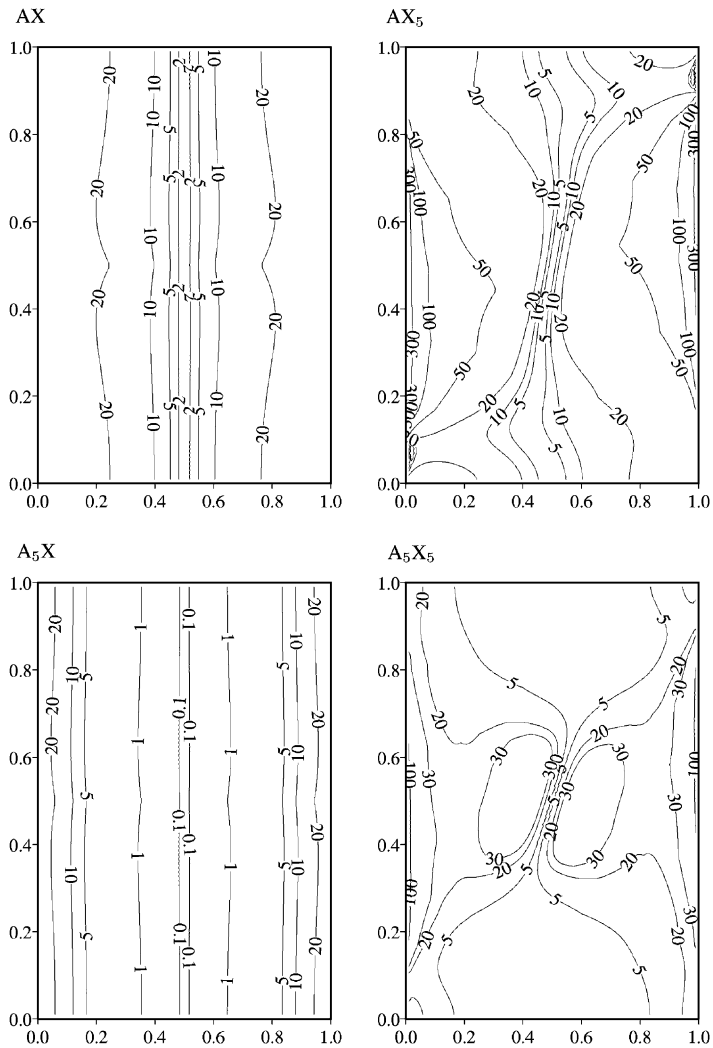

Fig. 11. Effect of the detector dead time on the isotopic ratio vs. the actual abundance of ^{m}A (horizontal axis) and $^{m'}$X (vertical axis). Base peak intensity is equal to 1 and $\tau = 0.03$ time units. The level curves indicate the values of δr (Eq. (6)).

6.5. Resolution

Fig. 13 encloses four contour maps with the absolute per-thousand deviation of the calculated A isotopic ratio from its expected value as a function of the actual ^{m}A and $^{m'}$X abundances for molecules A_5X, AX, AX_5, and A_5X_5. The same Gaussian peak shape used previously was applied.

In this example, the presence of the element X augments the interference of the mutual tail superposition. Similarly to the previous case, the effect is low when both elements have isotopes with the same abundances. This situation corresponds to the central point in the maps.

This trend can be understood by remembering that A has two isotopes whose masses differ by two mass units and X has two isotopes separated by one mass unit. Thus, for a lone A atom, the mutual tail effect is low. However, for A_pX_q species, the X atoms yield an isotopomeric pattern with one mass unit separated

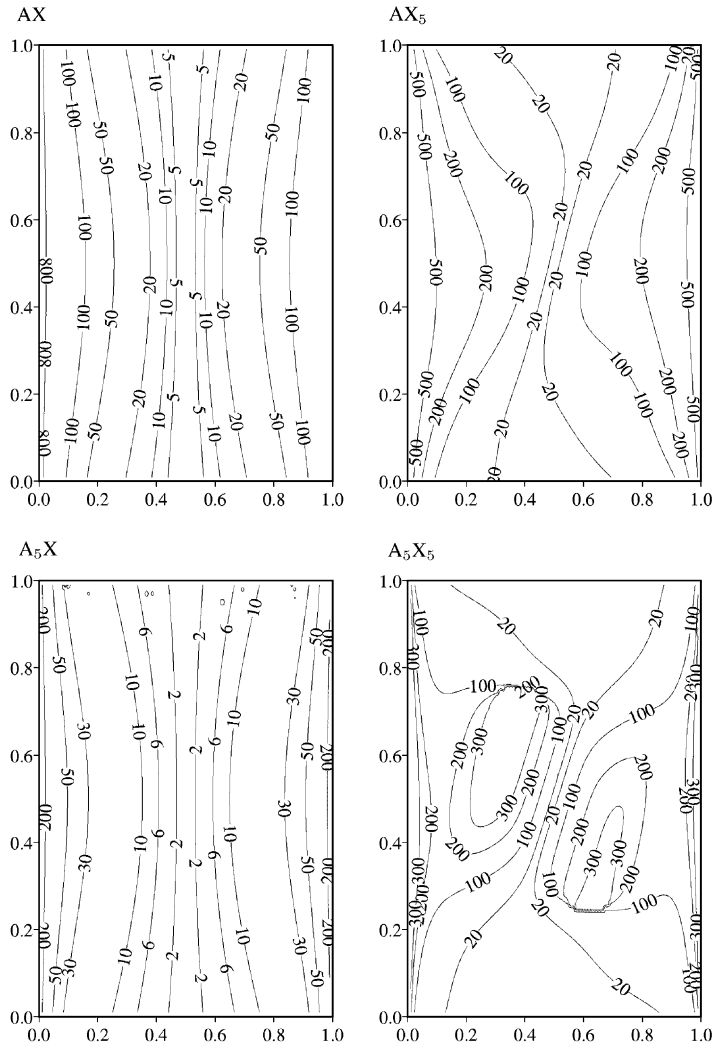

Fig. 12. Effect of the base line on the isotopic ratio vs. the actual abundance of ^{m}A (horizontal axis) and $^{m'}$X (vertical axis). Base peak intensity is equal to 1 and base line offset is 0.01. The level curves indicate the values of δr (Eq. (6)).

isotopomers. In this case, the mutual tail effect is more pronounced.

7. Utilization of selected peaks of a polyatomic cluster

As previously mentioned, one can use the IPDec method to determine the isotopic pattern of an element by selecting only some peaks of its cluster. In this section, this approach is demonstrated and its performance is evaluated. An extreme case was chosen: a hypothetical cluster corresponding to a C_{60} ion compared to the lone carbon atom.

Theoretically, the C_{60} cluster has 61 peaks. Thus, it is unreasonable to monitor all these peaks in order to determine, through IPDec method, the isotopic pattern of carbon. Nevertheless, one can obtain the carbon isotopic pattern by applying the IPDec method only to a few of these peaks.

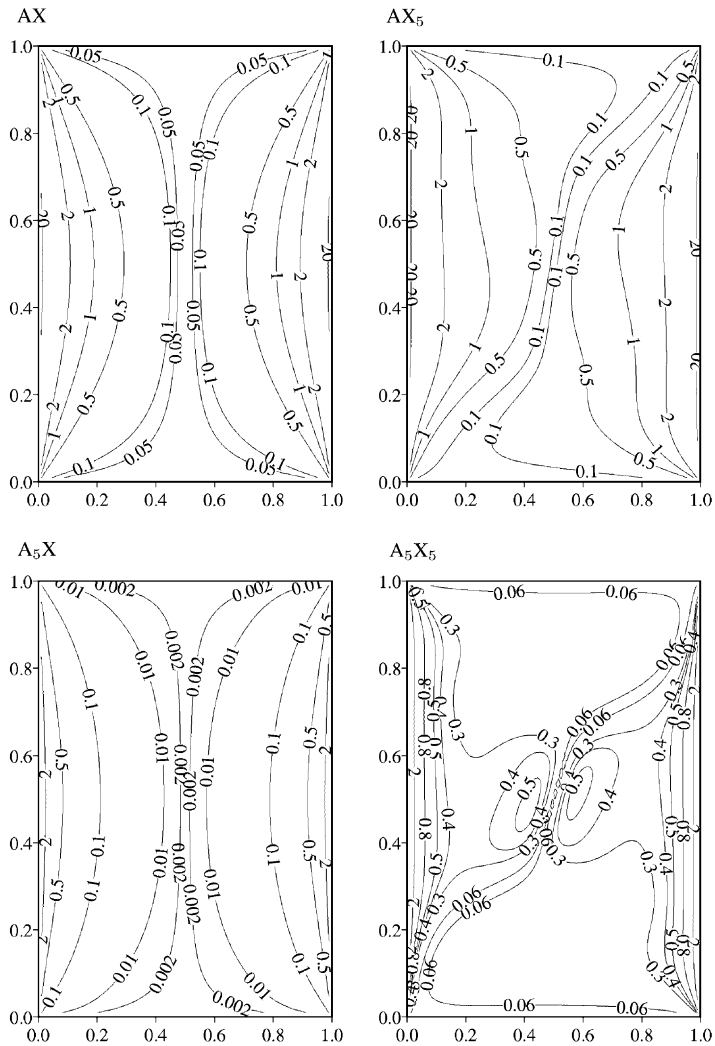

Fig. 13. Effect of the resolution on the isotopic ratio vs. the actual abundance of ^{m}A (horizontal axis) and $^{m'}$X (vertical axis). Gaussian-shaped peaks with σ equal to 0.25 u and integration window width equal to 0.1 u. The level curves indicate the values of δr (Eq. (6)).

The same non-idealities studied before are considered here for four cases: (1) the lone carbon atom, (2) the full C_{60} cluster, (3) the first eight peaks of the C_{60} cluster, and (4) the first two peaks of the C_{60} cluster. Case 1 corresponds to the classical approach. Case 2 corresponds to a hypothetical method, in which all the 61 peaks are monitored. Of course, this method is impracticable, but it is being considered for referential purposes. Case 3 is a more reasonable one, in which only the eight most intense peaks are monitored, and the reduced mass span decreases the probability of an isobaric interference. Case 4 is an extreme case, in which only the two most abundant peaks are considered. From the experimental standpoint, Case 4 is closely related to the conventional methods, where only two mass channels are monitored.

Homoscedastic and heteroscedastic data were considered. Standard deviations of the isotopic ratios were

determined over 10,000 point Monte Carlo runs. Homoscedastic data were simulated by applying errors drawn from a normal distribution with standard deviation equal to 1‰ of the cluster base peak. Heteroscedastic data were simulated by drawing errors for each peak from a normal distribution with relative standard deviation equal to 1‰.

For Case 1 (elemental ion), the standard deviation of the isotopic ratio was calculated using the error propagation formula

$$\sigma_{\text{ratio}} = \left(\frac{\sigma_{12}^2}{I_{13}^2} + \frac{I_{12}^2 \sigma_{13}^2}{I_{13}^4} \right)^{1/2} \quad (8)$$

where I_{12} and I_{13} are the intensities recorded at the ^{12}C and ^{13}C channels, respectively, and σ_{12} and σ_{13} are their respective standard deviations.

Instrumental mass discrimination effects were explored by multiplying each nominal peak intensity by 1.01^{m-m_0}, where m is the peak mass and m_0 is the mass of the first peak of the cluster. This corresponds to a 1% per mass unit positive exponential mass discrimination. The dead time (τ) was chosen so that $\tau I_{\text{base peak}} = 0.03$. Lack of spectral resolution was implemented by considering that each peak has a Gaussian shape with height equal to the nominal peak intensity, and standard deviation equal to 0.25 u, and integrating this function in a 0.1 u window around each nominal m/z values. Base line attribution error was considered by applying to each peak a positive offset equal to 1% of the cluster base peak.

Table 1 summarizes the effects of the main sources of systematic and random errors on the resulting $^{12}C/^{13}C$ isotopic ratio for simulated data. When the C_{60} approaches are compared, it is significant that Case 4 (two peaks) is never worse than either Cases 2 or 3. Mass discrimination has the same effect for all cases. On the other hand, the C_{60} approaches have better performance than elemental carbon for noise (homoscedastic data), detection non-linearity, baseline offset, and lack of resolution. It is worthy noting that Case 4 is never worse than the elemental carbon approach.

Of course, we are not suggesting that carbon isotopic analysis be performed through fullerene synthesis. Several practical problems, ranging from synthesis procedure to ionization method, would have to be treated. The idea is only to exemplify the alternatives opened by the IPDec method and show that it has no intrinsic disadvantage to conventional methods.

Table 1
Evaluation of systematic and random errors affecting the $^{12}C/^{13}C$ isotopic ratio obtained from a hypothetical C_{60} cluster compared to that one from the lone carbon atom[a]

Non-idealities	Lone carbon	C_{60} (all peaks)	C_{60} (first eight peaks)	C_{60} (first two peaks)
Noise (homoscedastic)[b]	17[h]	1.5	0.53	0.32
Noise (heteroscedastic)[c]	0.26[h]	1.0	0.37	0.26
Mass discrimination[d]	−9.9	−9.9	−9.9	−9.9
Detection non-linearity[e]	−29	−10	−10	−9.7
Base line[f]	−467	−12	−12	−4.9
Resolution[g]	−42	−0.60	−0.60	−0.58

[a] The considered $^{12}C/^{13}C$ ratio is 89.91 that corresponds to the natural carbon isotopic ratio.
[b] The results in this row are the per-thousand relative standard deviations of the isotopic ratio calculated by a 10,000-point Monte Carlo run using normal noise with standard deviation equal to 1‰ of the cluster base peak.
[c] The same as footnote b, but with standard deviation equal to 1‰ of the peak intensity.
[d] The results in this row are δr (Eq. (6)) for an exponential discrimination of 1% per u.
[e] Same as footnote d, but for a dead time such that its product by the base peak intensity equals 0.03.
[f] Same as footnote d, but for a base line offset equal to 1% of the base peak.
[g] Same as footnote d, but for Gaussian-shaped peaks with σ equal to 0.25 u and integration window width equal to 0.1 u.
[h] This value was analytically obtained by the error propagation formula (Eq. (8)) instead of Monte Carlo method.

8. Conclusions

Using IPDec method, one can obtain the isotopic pattern of one or more elements from the isotopomeric pattern of polyatomic species. The method enables one to use polyatomic species for the determination of isotopic patterns or isotopic ratios.

Of course, this computational treatment is more complex and time consuming than a simple division of two ion beam intensities. Moreover, the probability of isobaric interferences is greater for the soft ionization processes necessary to render polyatomic species. However, the flexibility to produce and select new species and the additional information obtained from partially or non-fragmented ions are issues that should be considered.

Analyses of random (noise) and systematic (base line, non-linearity, resolution, and mass discrimination) errors were carried out and shed light on some characteristics of the IPDec method. Of course, the results are primarily of theoretical importance, because for real applications several other practical issues, upon which the analyst has only partial control, will have to be tackled. The typical trends can be summarized as follows:

1. large numbers of A atoms tend to improve the performance of the polyatomic approach;
2. the X element can be deleterious if it is isotopically rich, but it can be useful as a “glue” element to obtain species with a large number of A atoms.

Our results suggest that the use of polyatomic and polyisotopic species does not a priori deteriorate the precision and accuracy of the obtained isotopic abundances.

Our modeling indicates that instrumental mass discrimination has the same effect upon the results obtained through the conventional and the polyatomic approach. This result is not intuitive and suggests that strategies based on large-mass clusters might perform better than conventional ones, because instrumental mass bias is smaller in the large m/z region.

Of course, polyatomic species, by definition, have more isotopomeric peaks than monatomic ones, which can lead one to question the viability of the approach, because of the greater number of mass channels to be monitored. However, only the most intense peaks of the cluster must be monitored, and this can lead to rather impressive results.

Although several cases show that it can indeed be better to work with polyatomic species and the IPDec method than to stick to the monatomic approach, the aim of these comparisons was not to prove that our method is always better than any of the conventional techniques. On the other hand, the opposite cannot be stated a priori either. The final decision about which method one should use for a specific analysis must be based on the figures of merit of the analytical process as a whole, rather than on unsound preconceived notions.

Acknowledgements

This work had financial support from Fundação de Amparo à Pesquisa do Estado de São Paulo (FAPESP) and Conselho Nacional de Desenvolvimento Científico e Tecnológico (CNPq). Authors thank CNPq and FAPESP for fellowships, Miss M.C.B. Moraes for electrospray mass spectra, and Miss A.D. Richter for the English revision.

References

[1] U. Gießmann, U. Greb, Fr. J. Anal. Chem. 350 (1994) 186.
[2] W.A. Brand, J. Mass Spectrom. 31 (1996) 225.
[3] J.R. Bacon, J.S. Crain, A.W. McMahon, J.G. Williams, J. Anal. At. Spectrom. 12 (1997) R407.
[4] S. Tonarini, M. Pennisi, W.P. Leeman, Chem. Geol. 142 (1997) 129.
[5] A.J. Spivak, J.M. Edmond, Anal. Chem. 58 (1986) 31.
[6] M.C.B. Moraes, J.G.A. Brito-Neto, C.L. Lago, Int. J. Mass Spectrom. 198 (2000) 121.
[7] P.D.P. Taylor, S. Lehto, S. Valkiers, P. De Bievre, O. Selgrad, U. Flegel, T. Kruck, Anal. Chem. 70 (1998) 1033.
[8] K.G. Heumann, S.M. Gallus, G. Radlinger, J. Vogl, J. Anal. At. Spectrom. 13 (1998) 1001.
[9] B.D. Holt, N.C. Sturchio, T.A. Abrajano, L.J. Heraty, Anal. Chem. 69 (1997) 2727.

[10] B.P. Datta, P.S. Khodade, A.R. Parab, A.H. Goyal, S.A. Chitambar, H.C. Jain, Int. J. Mass Spectrom. Ion Proc. 116 (1992) 87.
[11] B.P. Datta, P.S. Khodade, A.R. Parab, A.H. Goyal, S.A. Chitambar, H.C. Jain, Rapid Commun. Mass Spectrom. 7 (1993) 581.
[12] B.P. Datta, P.S. Khodade, A.R. Parab, S.A. Chitambar, H.C. Jain, Int. J. Mass Spectrom. Ion Proc. 142 (1995) 69.
[13] B.P. Datta, Rapid Commun. Mass Spectrom. 14 (2000) 706.
[14] B.P. Datta, Rapid Commun. Mass Spectrom. 14 (2000) 1571.
[15] H. Kubinyi, Anal. Chim. Acta 247 (1991) 107.
[16] W.H. Press, S.A. Teukolsky, W.T. Vetterling, B.P. Flannery Numerical Recipes in C: The Art of Scientific Computing, 2nd Edition, Cambridge University Press, Cambridge, 1996, p. 408.
[17] S.R. Hart, A. Zindler, Int. J. Mass Spectrom. Ion Proc. 89 (1989) 287.
[18] A. Held, P.D.P. Taylor, J. Anal. At. Spectrom. 14 (1999) 1075.
[19] K.F. Blom, Org. Mass Spectrom. 23 (1988) 194.
[20] A.L. Rockwood, S.L. Van Orden, Anal. Chem. 68 (1996) 2027.